



ELSEVIER

Journal of Power Sources 93 (2001) 145–150

JOURNAL OF  
POWER  
SOURCES

www.elsevier.com/locate/jpowersour

## Characteristics of a lithium-polymer battery based on a lithium powder anode

C.W. Kwon<sup>a</sup>, S.E. Cheon<sup>b</sup>, J.M. Song<sup>c</sup>, H.T. Kim<sup>d,\*</sup>, K.B. Kim<sup>c</sup>, C.B. Shin<sup>a</sup>, S.W. Kim<sup>b</sup>

<sup>a</sup>Department of Chemical Engineering, Ajou University, Wonchon-dong Paldal-gu, Suwon, Kyonggi-do 442-749, South Korea

<sup>b</sup>Department of Molecular Science and Technology, Ajou University, Wonchon-dong Paldal-gu, Suwon, Kyonggi-do 442-749, South Korea

<sup>c</sup>NESS Co., Ltd., 29-9 Wonchon-dong, Paldal-gu, Suwon, Kyonggi-do 442-380, South Korea

<sup>d</sup>Institute for Advanced Engineering, 29-9 Wonchon-dong, Paldal-gu, Suwon, Kyonggi-do 442-380, South Korea

Received 6 May 2000; accepted 14 August 2000

### Abstract

The characteristics of a lithium-polymer battery which comprises a novel lithium powder-based anode, a LiCoO<sub>2</sub>-based cathode, and a polyacrylonitrile-based gel-type polymer electrolyte are investigated. Lithium powder with diameter of 20–40 μm is produced by forming a dispersion of molten lithium metal in hot silicon oil and subsequent cooling. The lithium powder electrode is successfully manufactured by coating the slurry of the lithium powder, PVdF binder, and THF on a copper substrate. A lithium-polymer cell with the lithium powder anode shows somewhat longer cycle life at a 1 C rate of discharge and higher discharge capacity at low temperature compared with a cell prepared with a lithium foil anode. A reduction of polarization due to the large surface area of the lithium powder anode is believed to be responsible for these characteristics. © 2001 Elsevier Science B.V. All rights reserved.

**Keywords:** Lithium powder anode; Lithium foil anode; Lithium-polymer battery; Solid polymer electrolyte; Interfacial resistance

### 1. Introduction

Lithium metal is extremely attractive as a negative electrode (anode) material for secondary batteries due to its low atomic weight (6.94), high negative electrode potential (−3.03 V versus standard hydrogen electrode), and high specific capacity (3.86 A h g<sup>−1</sup>). These advantages which are possessed by no other metal are responsible for the development of the so-called ‘lithium battery’. Lithium metal has not been widely used in secondary batteries, however, because of its low rechargeability due to a non-faradaic chemical reaction with non-aqueous electrolytes and the formation of lithium dendrites during the charging process that lead to short-circuiting of cells. For these reasons, a carbon anode in which Li can be intercalated is employed in lithium-ion batteries as an alternative to a lithium metal anode.

Nevertheless, the use of lithium metal as an anode is still a matter of interest because a new cathode material, namely, sulfur-based organic material with much higher capacity has been suggested [1–3], and the capacity of the carbon anode might be insufficient for such an advanced cathode material.

Many attempts have been made to modify the morphology of the lithium deposits and to improve the cycling efficiency by forming a dense and compact passivation layer between lithium metal anodes and solid polymer electrolytes (SPE). These include the use of a more inert solvent mixture [4,5], novel electrolyte salts [5,6], the control of pre-cycling [7,8], and the addition to the electrolyte of compounds such as hydrofluoric acid [9], poly(ethylene glycol) dimethyl ether (PEGDME) [10], aluminum iodide (AlI<sub>3</sub>) [11–13], magnesium iodide (MgI<sub>2</sub>) [13], CO<sub>2</sub> [14,15], and perfluoropolyether (PFPE) [16].

In this work, we suggest a novel anode based on lithium powder for lithium secondary batteries. Compared with lithium foil, it can provide higher active surface area, and thus, the polarization of lithium ions concentrated on the active lithium surface will be lower at the same current. As a consequence, the charge transfer rate at the lithium anode can be increased. To realize this idea, we have prepared the lithium powder by forming a dispersion of molten lithium metal in hot silicon oil, followed by rapid cooling of the dispersion. The lithium powder anode is manufactured by coating the slurry of lithium powder and an appropriate binder on to a Cu foil current-collector. To our best knowledge, it is the first study that demonstrates the realization of a lithium powder anode, and a lithium-polymer battery which

\* Corresponding author. Tel.: +82-31-219-0636; fax: +82-31-219-0610.  
E-mail address: htkim@iae.re.kr (H.T. Kim).

employs it. The characteristics of the lithium powder anode are investigated by means of cyclic voltammetry and ac impedance spectroscopy. For comparison, the performance of a lithium-polymer battery prepared with a lithium foil anode is evaluated.

## 2. Experimental

All experiments were conducted under dry condition (dew point is  $-50^{\circ}\text{C}$ ).

### 2.1. Preparation of lithium powder

Lithium powder was prepared by forming a dispersion of lithium melted in hot silicon oil ( $245^{\circ}\text{C}$ ) with a homogenizer at 25,000–30,000 rpm, and subsequent cooling under atmospheric conditions. The dispersion of fine solid lithium powder was filtered, and the filtered powder was washed five times with cyclo-hexane (Aldrich). The resulting powder was dried at room temperature for 5 h and sieved with a mesh. The particle size ranged between 20 and 40  $\mu\text{m}$ .

### 2.2. Preparation of lithium metal powder electrode

The lithium powder slurry was prepared by mixing 5 g of lithium powder, 0.75 g of PVdF binder, and 13.5 ml of anhydrous THF with stirring for 1 h at room temperature. The viscous slurry was coated on copper foil (thickness: 10  $\mu\text{m}$ ) with an applicator (depth: 300  $\mu\text{m}$ ). The size of the anode was 25 mm  $\times$  40 mm.

### 2.3. Preparation of lithium foil electrode

Lithium foils (23 mm  $\times$  37 mm) were laminated on both sides of a copper mesh. The resulting stack of lithium foil and copper mesh was pressed by using a rolling machine to impart good adhesion between the current-collector and the lithium foil.

### 2.4. Preparation of polymer electrolyte

To 36 g of a 1 M  $\text{LiPF}_6$  solution of EC/DMC/GBL mixture (2:1:1 by weight), 6 g of polyacrylonitrile (PAN) was added. The mixture was heated at  $160^{\circ}\text{C}$  for 40 min to form a homogeneous solution. This solution was then coated on Mylar<sup>®</sup> film with an applicator (gap: 200  $\mu\text{m}$ ).

### 2.5. Cell fabrication

Lithium-polymer cells were fabricated by stacking the anode, the cathode and the polymer electrolyte. The polymer electrolytes were laminated on both sides of the lithium anode, and then the cathode was attached to each side of the assembly. The cell configuration is shown in Fig. 1. The resulting stack was sealed with an aluminum-coated plastic pack under vacuum.

### 2.6. Cell testing

The charge and discharge characteristics were investigated by using a MACCOR 4000 battery cycler. The test cell was charged at a constant current for a given time with an upper potential limit of 4.2 V, and then discharged at a constant current with a cut-off voltage of 3.0 V. To measure the discharge capacity at low temperature, the fully charged cell was equilibrated at the test temperature for 1 h, and the discharge was proceeded at the test temperature.

### 2.7. ac impedance measurements

The ac impedance of the cell was determined with a IM6 impedance analyzer. The data were transmitted from the analyzer to a personal computer through GPIB. The frequency range and amplitude were set at 50 m to 1 MHz and 5 mV, respectively. All electrical measurements were made at open-circuit voltage. The interfacial resistance was determined from the complex impedance diagram.

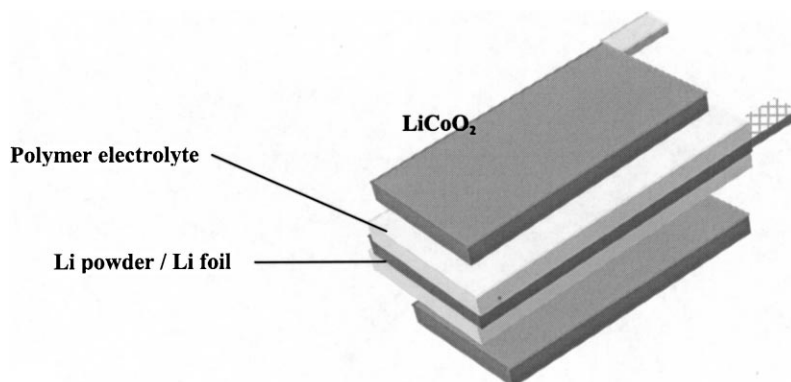


Fig. 1. Configuration of test cell.

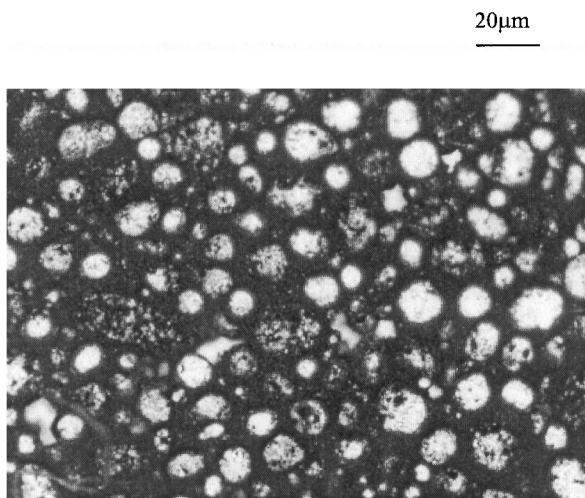


Fig. 2. Optical microscopic image of Li powder electrode.

### 3. Results and discussion

#### 3.1. Characterization of lithium powder electrode

An optical microscopic image of the lithium powder anode is shown in Fig. 2. The spherical lithium particles are dispersed uniformly in the anode. The average lithium particle size is 20  $\mu\text{m}$ . With a PVdF binder, the lithium powder adheres well to the current-collector.

The voltammetric behavior of the lithium powder electrode and the lithium foil electrode is compared in Fig. 3. Both cells consist of two electrodes using a lithium foil or a lithium powder electrode as a reference and a counter electrode, and  $\text{LiCoO}_2$  electrode as a working electrode. The lithium powder cell shows a sharper anodic slope in the voltage range 3.9–4.2 V, and also a higher cathodic peak at 3.6 V, compared with the lithium foil cell. This can be explained in terms of the difference in surface area of the

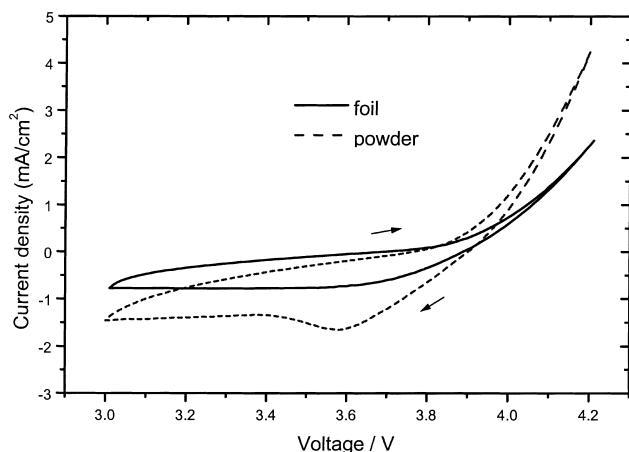


Fig. 3. Cyclic voltammograms for Li powder and Li foil cells after 30 cycles at 0.2 C (scan rate: 10  $\text{mV s}^{-1}$ ).

Table 1

Charging end-voltage with cycle number of Li foil cell and Li powder cell cycled at the 0.2 C rate

Cell type	1st (V)	5th (V)	10th (V)	15th (V)	20th (V)
Li foil	4.09	4.10	4.10	4.09	4.10
Li powder	4.01	4.02	4.02	4.03	4.06

anode. The specific area of the lithium powder electrode is larger than that of the lithium foil anode, even though both electrodes have the same dimensions. Since lithium deposition and dissolution are surface reactions, the increase of active surface area results in an increase in the electrochemical reaction rate at the lithium surface and a decrease of polarization of lithium ions at the interface between the electrolyte and the electrode.

The above results imply that upon charging with a constant current, the voltage of the lithium powder cell would increase more slowly than that of the lithium foil cell and, furthermore, the charge capacity would be higher at the same end-voltage for charging. A comparison is given in Table 1 of the voltage at the end of charging process at constant current with constant cut-off time for the lithium powder and foil cells as a function of cycle number. These cells were charged at the 0.2 C rate for 5 h and discharged at the 0.2 C rate with a cut-off voltage of 3.0 V. Since the charging current and time were fixed, the charge capacity of the both cells was the same. The lithium powder cell showed a much lower charge end-voltage which is in good agreement with the above observations. The decreased polarization of lithium ions on the interface between the polymer electrolyte and the lithium powder electrode could result in a decrease of overpotential and, consequently, a decrease of cell voltage with the same charging capacity. On the first cycle, the difference in end-voltage is about 80 mV. The charge end-voltage increases with cycle number for the lithium powder cell which indicates an increase in cell resistance. This is attributed to the formation of a passivation layer on the surface of the lithium metal powder during cycling.

Fig. 4(a) and (b) show the voltammograms before and after 30 cycles of repeated charge and discharge at the 0.2 C rate for a lithium foil and a lithium powder cell, respectively. The lithium foil electrode shows a dramatic change in the shape of the curve after 30 cycles. This strongly indicates that the surface of the lithium foil electrode becomes rough during repeated cycling. The concentrated deposition of lithium ions on a specific area of the lithium foil and the corrosive reaction between deposited Li and impurities occurs, and results in a porous morphology. For the lithium powder cell, both the cathodic and the anodic currents increase upon repeated cycling but the change is less significant than for the lithium foil cell. Since the lithium powder electrode is originally porous before cycling, the morphological change during cycling is relatively small. It should be noted that the lithium powder cell displays a much

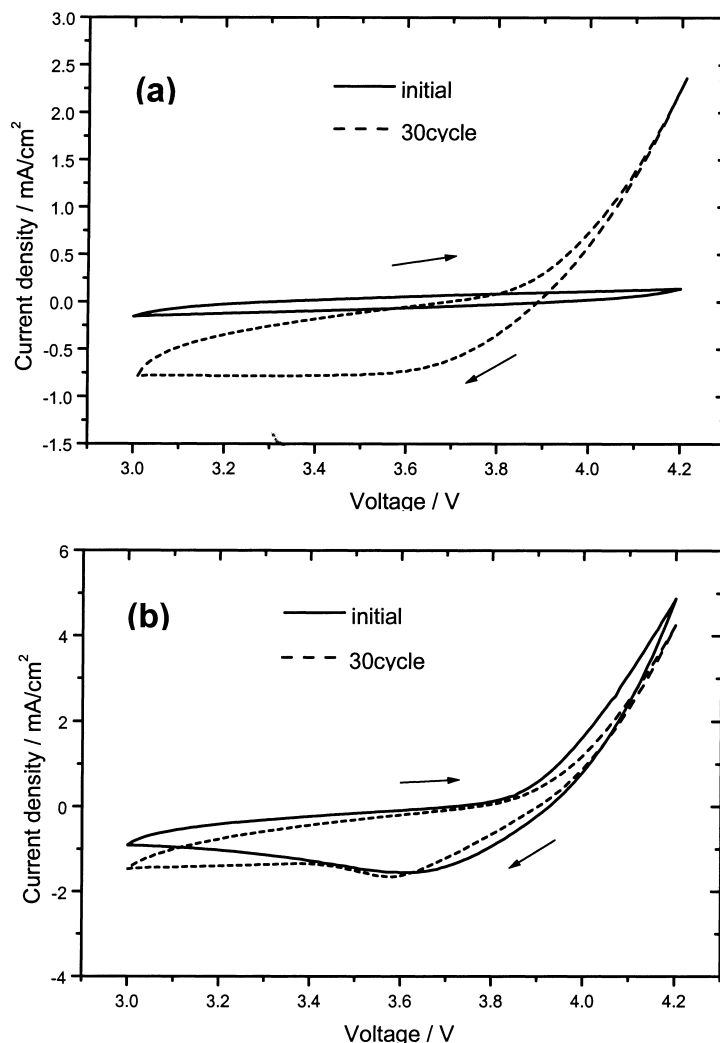


Fig. 4. Cyclic voltammograms of (a) Li foil cell and (b) Li powder cell before and after 30 cycles (scan rate:  $10 \text{ mV s}^{-1}$ ).

higher current density in the voltammogram even after 30 cycles than the lithium foil cell. This suggests that the morphological differences remain between the lithium foil and the lithium powder cells after 30 cycles.

### 3.2. Change of interfacial resistance of lithium powder cell during repeated cycling

To examine the stability of lithium powder electrode, impedance measurements of the  $\text{LiCoO}_2/\text{SPE}/\text{Li}$  cells were performed. From the diameter of the first semi-circle found in the complex impedance spectra, the interfacial resistance of the cell is determined. Although, the resistance includes contributions from both the cathode and the anode, it is dominated by the characteristics of the interface between the lithium anode and the polymer electrolyte. This is explained by the much higher interfacial resistance for the  $\text{LiCoO}_2/\text{SPE}/\text{Li}$  cell compared with that for the  $\text{LiCoO}_2/\text{SPE}/\text{carbon}$  cell.

We investigated the change in the interfacial resistance during repeated cycling at the 0.2 and 1 C rates for the lithium foil and the lithium powder cells. The results are presented in Fig. 5. Irrespective of the charge–discharge rate, the powder cell shows a much lower interfacial resistance. Facile lithium deposition and dissolution would explain this behavior. At the 0.2 C rate, the interfacial resistance of the lithium foil cell exponentially increases with cycle number. By contrast with the lithium foil cell, the lithium powder cell exhibits a rather stable interfacial resistance during cycling. During the course of repeated charge and discharge at the 1 C rate, the interfacial resistance of the lithium foil cell continuously increases and then starts to decrease at 20–30 cycles. The decrease is thought to be due to a minor short. This short seems to come from non-homogeneous current distribution which result in dendritic growth during lithium deposition. By contrast, the lithium powder cell does not show any evidence of shorting, even at the 1 C rate.

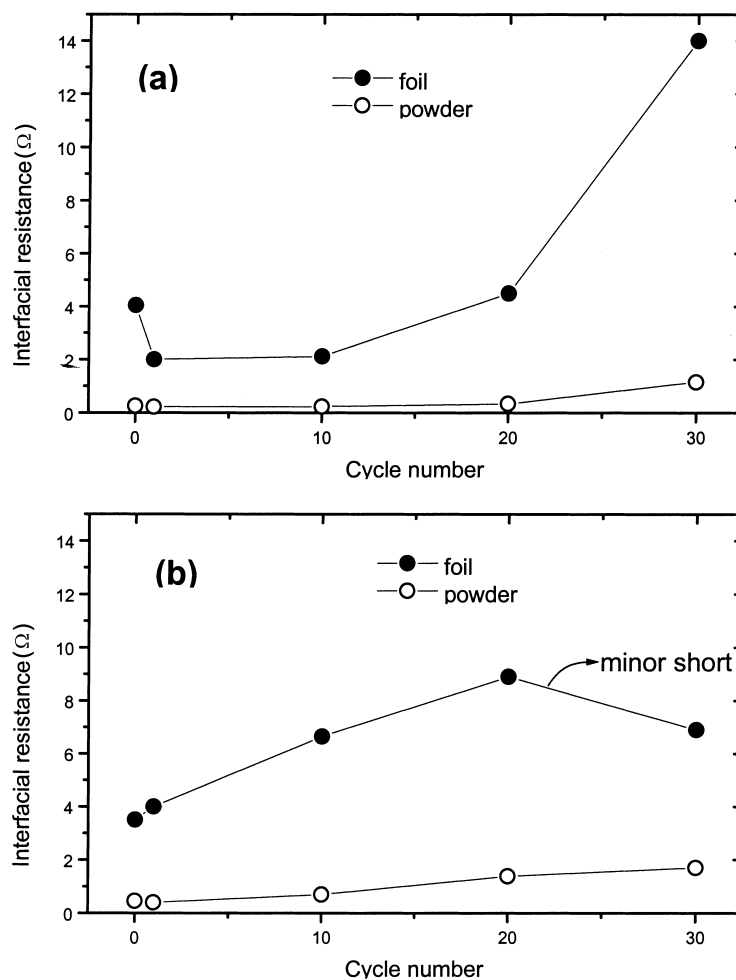


Fig. 5. Interfacial resistance of Li foil and Li powder cells upon cycling at (a) 0.2 C and (b) 1 C.

### 3.3. Cycling efficiency of lithium powder cell

The cycling efficiencies for the lithium foil and the lithium powder cells are shown in Fig. 6. The cycling efficiency at the 1 C rate reaches more than 95% which is

even higher than that at the 0.2 C rate, for both the lithium foil and the lithium powder cells. A considerable difference between the lithium powder and the lithium foil cells can be found above 20 cycles at the 1 C rate. The lithium powder cell displays higher cycling efficiency in this regime.

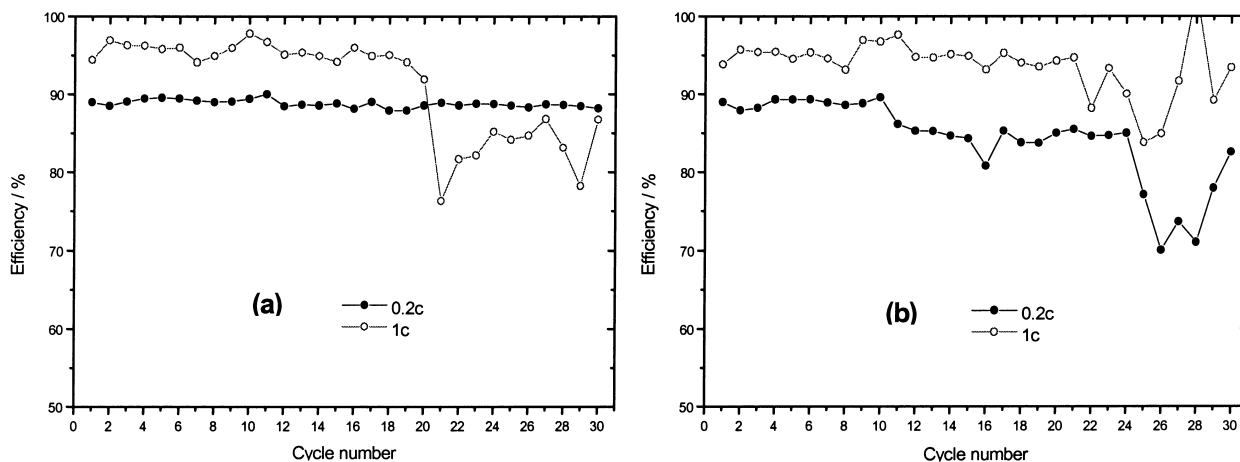


Fig. 6. Cycling efficiency as function of cycle number for (a) Li foil cell and (b) Li powder cell.

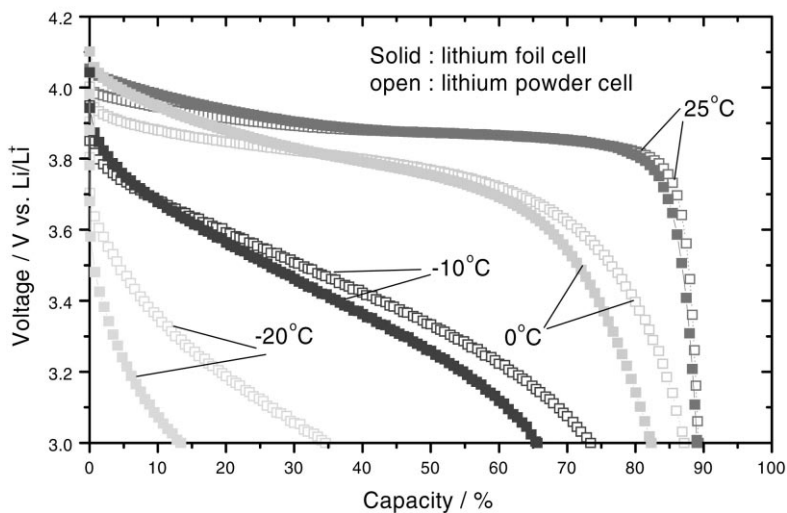


Fig. 7. Voltage profile of Li foil cell and Li powder cell during discharge at different temperatures (discharge rate: 0.2 C).

The difference in the cycling efficiency, at various C rates, between the lithium foil and the lithium powder cells can be explained in terms of a difference in the specific surface area of the anodes. Since both the lithium foil and the lithium powder anodes have high reactivity with the electrolyte or with impurities such as water and oxygen, the reaction rate of the lithium with electrolyte depends on the surface area of Li which makes a contact with electrolyte. Therefore, it can be reasonably expected that the reaction between the surface of the lithium and the electrolyte or a impurity would be more severe for a lithium powder anode than for a lithium foil anode. At high charge–discharge rates, the rate of lithium deposition/dissolution could be faster than the reaction rate between lithium and impurities or the electrolyte. For this reason, the merit of high specific area of the lithium powder anode could appear at high rate. With decrease in charge rate, ‘dead’ lithium formation which lowers cycling efficiency becomes more significant, and would be greater for the lithium powder anode because of the larger specific surface area. Indeed, we have observed that a larger amount of black dead lithium was produced on the lithium powder anode after cycling at 0.2 C than on the lithium foil anode. On the other hand, at the 1 C rate, the lithium powder anode develops less dead lithium than the lithium foil after the repeated cycling.

#### 3.4. Thermal characteristics of lithium powder cell

The voltage profiles during discharge for the lithium foil and the lithium powder cells at the 0.2 C rate and various temperatures are shown in Fig. 7. The test cells were charged at the 0.2 C rate at room temperature, stored at the test temperature for 1 h, and then discharged at the test temperature. It is found that the lithium powder cells are superior to lithium foil cells at low temperatures (0, –10, and –20°C) while both cells show similar discharging capacity at room temperature. At –20°C, the discharge capacities of

the lithium powder and the lithium foil cells are 35 and 13%, respectively. Low discharge capacity at low temperature is generally caused by high polarization of the lithium ions at the interface between the electrolyte and the electrode. Because of the larger surface area of the lithium powder anode, the rate of dissolution is higher, and leads to lower polarization and, consequently, higher discharge capacity at such low temperatures.

#### References

- [1] K. Naoi, K. Kawase, M. Mori, M. Komiyama, J. Electrochem. Soc. 144 (1997) L173.
- [2] T. Sotomura, T. Tatsuma, N. Oyama, J. Electrochem. Soc. 143 (1996) 3152.
- [3] K. Naoi, K. Kawase, M. Mori, Y. Inoue, J. Electrochem. Soc. 144 (1997) L170.
- [4] S.S. Zhang, C.A. Angell, J. Electrochem. Soc. 143 (1996) 4047.
- [5] X. Wang, E. Yasukawa, S. Mori, J. Electrochem. Soc. 146 (1999) 3992.
- [6] K. Naoi, M. Mori, Y. Naruoka, W.M. Lamanna, R. Atanasoski, J. Electrochem. Soc. 146 (1999) 462.
- [7] M. Ishikawa, Y. Takaki, M. Morita, Y. Matsuda, J. Electrochem. Soc. 144 (1997) L90.
- [8] T. Sotomura, K. Adachi, M. Taguchi, M. Iwaku, T. Tatsuma, N. Oyama, J. Power Sources 81 (1999) 192.
- [9] S. Shiraishi, K. Kanamura, Z. Takehara, J. Appl. Electrochem. 25 (1995) 584.
- [10] M. Mori, Y. Naruoka, K. Naoi, J. Electrochem. Soc. 145 (1998) 2340.
- [11] M. Ishikawa, K. Otani, M. Morita, Y. Matsuda, Electrochim. Acta 41 (1996) 1253.
- [12] M. Ishikawa, M. Morita, Y. Matsuda, J. Power Sources 68 (1997) 501.
- [13] M. Ishikawa, S. Machino, M. Morita, J. Electroanal. Chem. 473 (1999) 279.
- [14] H. Gan, E.S. Takeuchi, J. Power Sources 62 (1996) 45.
- [15] T. Osaka, T. Momma, T. Tajima, Y. Matsumoto, J. Electrochem. Soc. 142 (1995) 1057.
- [16] E. Eweka, J.R. Owen, A. Ritchie, J. Power Sources 65 (1997) 247.